Feasibility of single-source dual-energy computed tomography for urinary stone characterization and value of iterative reconstructions

Morsbach, Fabian ; Wurnig, Moritz C ; Müller, Daniel ; Krauss, Bernhard ; Korporaal, Johannes Georg ; Alkadhi, Hatem

Abstract: PURPOSE: The purposes of this study were to demonstrate the feasibility and accuracy of single-source dual-energy (DE) computed tomography (CT) with sequential data acquisition and a coregistration motion correction algorithm for urinary stone characterization and to evaluate the value of iterative reconstructions (IRs) in DE imaging. MATERIALS AND METHODS: Thirty-five urinary stones were placed in cylindrical phantoms with diameters of 30 and 40 cm. The phantoms were scanned on a 64-section CT machine with a single-source DE protocol consisting of 2 sequential acquisitions at 80 and 140 kilovolt (peak). The phantom was moved between the 80- and 140-kilovolt (peak) scans. Images were reconstructed with weighted filtered back projection (FBP) and with IR, and data were coregistered. Two independent and blinded readers assessed data sets for stone detection, overall image quality, and visibility of stones. Image noise and Hounsfield unit values of the stones were measured, and the DE index was calculated. In addition, the data sets were analyzed on color-coded images using the standard postprocessing software for differentiating uric acid- (UA) from non-UA-containing stones. RESULTS: The motion correction algorithm achieved a good coregistration of the 2 scans with different energy levels. Both readers detected all stones on all data sets with both reconstruction types. The overall image quality was rated significantly higher in IR images in the 40-cm phantom as compared with that in FBP images ($P < 0.05$), whereas no significant difference was found for the 30-cm phantom. Visibility of stones was rated significantly higher for both the 30- and 40-cm phantoms on IR as compared with that on FBP images, an effect that was pronounced for UA stones ($P < 0.05$). Noise was significantly reduced by up to 31% in the 40-cm phantom when using IR as compared with FBP ($P < 0.001$). The DE index was similar in the FBP and IR data sets for the 30- ($P = 0.116$) and 40-cm phantoms ($P = 0.544$), being significantly different between UA-containing stones, cystine, and struvite stones as well as stones of other compositions ($P < 0.001$). The postprocessing software classified all stones correctly as UA- or non-UA-containing stones on color-coded images. In the 40-cm phantom, false-positively colored voxels were found in the FBP data sets, which were not seen when using IR instead. CONCLUSIONS: Our study indicates that single-source dual-energy CT with sequential acquisitions at different energy levels and a coregistration motion correction algorithm is feasible and accurate for characterizing urinary stone composition on the basis of phantom evaluation. As compared with reconstructions with FBP, the use of IR in dual-energy CT reduces noise, improves overall image quality and visibility of stones particularly in large phantoms, and helps to avoid false classifications of urinary stones.

DOI: https://doi.org/10.1097/RLI.0000000000000002

Originally published at:
Morsbach, Fabian; Wurnig, Moritz C; Müller, Daniel; Krauss, Bernhard; Korporaal, Johannes Georg; Alkadhi, Hatem (2014). Feasibility of single-source dual-energy computed tomography for urinary stone characterization and value of iterative reconstructions. Investigative Radiology, 49(3):125-130.
DOI: https://doi.org/10.1097/RLI.0000000000000002

Feasibility of Single-Source Dual-Energy Computed Tomography for Urinary Stone Characterization and Value of Iterative Reconstructions

Fabian Morsbach, MD, Moritz C. Wurnig, MD, MSc,* Daniel Müller, PhD,† Bernhard Krauss, PhD,‡ Johannes Georg Korporaal, PhD,‡ and Hatem Alkadhi, MD, MPH, EBCR**

Purpose: The purposes of this study were to demonstrate the feasibility and accuracy of single-source dual-energy (DE) computed tomography (CT) with sequential data acquisition and a coregistration motion correction algorithm for urinary stone characterization and to evaluate the value of iterative reconstructions (IRs) in DE imaging.

Materials and Methods: Thirty-five urinary stones were placed in cylindrical phantoms with diameters of 30 and 40 cm. The phantoms were scanned on a 64-section CT machine with a single-source DE protocol consisting of 2 sequential acquisitions at 80 and 140 kilovolt (peak). The phantom was moved between the 80– and 140–kilovolt (peak) scans. Images were reconstructed with weighted filtered back projection (FBP) and with IR, and data were coregistered. Two independent and blinded readers assessed data sets for stone detection, overall image quality, and visibility of stones. Image noise and Hounsfield unit values of the stones were measured, and the DE index was calculated. In addition, the data sets were analyzed on color-coded images using the standard postprocessing software for differentiating uric acid- (UA) from non–UA-containing stones.

Results: The motion correction algorithm achieved a good coregistration of the 2 scans with different energy levels. Both readers detected all stones on all data sets with both reconstruction types. The overall image quality was rated significantly higher in IR images in the 40-cm phantom as compared with that in FBP images ($P < 0.05$), whereas no significant difference was found for the 30-cm phantom. Visibility of stones was rated significantly higher for both the 30- and 40-cm phantoms on IR as compared with that on FBP images, an effect that was pronounced for UA stones ($P < 0.05$). Noise was significantly reduced by up to 31% in the 40-cm phantom when using IR as compared with FBP ($P < 0.001$). The DE index was similar in the FBP and IR data sets for the 30- ($P = 0.116$) and 40-cm phantoms ($P = 0.544$), being significantly different between UA-containing stones, cystine, and struvite stones as well as stones of other compositions ($P < 0.001$). The postprocessing software classified all stones correctly as UA- or non–UA-containing stones on color-coded images. In the 40-cm phantom, false-positively colored voxels were found in the FBP data sets, which were not seen when using IR instead.

Conclusions: Our study indicates that single-source dual-energy CT with sequential acquisitions at different energy levels and a coregistration motion correction algorithm is feasible and accurate for characterizing urinary stone composition on the basis of phantom evaluation. As compared with reconstructions with FBP, the use of IR in dual-energy CT reduces noise, improves overall image quality and visibility of stones particularly in large phantoms, and helps to avoid false classifications of urinary stones.

Received for publication May 24, 2013; and accepted for publication, after revision, August 27, 2013.

From the *Institute of Diagnostic and Interventional Radiology, †Institute of Clinical Chemistry, University Hospital Zurich, Zurich, Switzerland; and ‡Siemens AG, Healthcare Sector, Imaging & Therapy Systems, Forchheim, Germany.

Conflicts of interest and sources of funding: B.K. and J.G.K are employees of Siemens Healthcare.

Reprints: Hatem Alkadhi, MD, MPH, EBCR, Institute of Diagnostic and Interventional Radiology, University Hospital Zurich, Raemistrasse 100, CH-8091 Zurich, Switzerland. E-mail: hatem.alkadhi@usz.ch.

ISSN: 0020-9996/14/4903–0125

Key Words: urinary stones, dual-energy, computed tomography, motion correction

(*Invest Radiol* 2014;49: 125–130)

Computed tomography (CT) represents the imaging modality of choice for the detection of urinary stones.[1,2] Further characterization of stones based on their attenuation values, however, has repetitively shown to be possible with only limited accuracy.[3–5] The recent introduction of dual-energy CT has resulted in improvements for stone characterization, particularly in the differentiation of uric acid (UA)- and non-UA–containing stones.[6–10] Until recently, 2 techniques have been commercially available for dual-energy CT imaging, that is, the dual-source principle with the simultaneous acquisition of data sets at 2 different energy levels[6–10] and the rapid kilovoltage switching technique, which is used by specific single-source CT scanners.[11,12] The drawback of both of these techniques, however, is the requirement for dedicated CT machines that are capfable of dual-energy imaging. With a conventional single-source CT scanner, dual-energy CT is usually not feasible with adequate quality and performance.

Weighted filtered back projection (FBP) has been the standard reconstruction technique in CT imaging for decades. With increasing computational power, iterative reconstruction (IR) has recently become available with sufficient speed, allowing its integration into daily clinical routine. Iterative reconstruction can be used for improving image quality by reducing noise or for reducing radiation dose while maintaining image quality.[13–16] Application of IR instead of FBP reconstructions has shown value also in patients with obesity, allowing for a radiation dose reduction of approximately 32% while maintaining a diagnostic image quality.[13]

Given that previous dual-energy CT studies showed limited accuracy regarding urinary stone detection in patients with abdominal obesity mainly because of the increase in noise,[17–19] which can be explained by the stronger absorption of the 80–kilovolt (peak) (kV[p]) spectrum in these patients, a reduction in noise such as that observed with IR would be desirable for dual-energy CT applications as well.

Thus, the purpose of this ex vivo study was 2-fold: first, to evaluate the feasibility and accuracy of single-source dual-energy CT (DECT) with sequential data acquisition and using a coregistration motion correction algorithm for urinary stone characterization, with x-ray diffraction as the standard of reference; and second, to evaluate the value of IR in DECT imaging about stone visualization and image quality in phantoms of different sizes.

MATERIALS AND METHODS

Phantom

Thirty-five urinary stones were collected through straining, endoscopic retrieval, or surgical intervention during clinical routine. The stones were characterized with the x-ray diffraction method, and

the stone size was measured with a precision caliper. A maximum of 5 stones were inserted in a kidney-equivalent density substance by wrapping the stones in flattened meat. Then, the phantoms were placed in custom-made cylindrical water-equivalent phantoms (Quality Assurance in Radiology and Medicine, Moehrendorf, Germany) representing a normal-sized (diameter, 30 cm) patient and a patient with obesity (diameter, 40 cm) (Fig. 1).

Computed Tomographic Data Acquisition and Reconstruction

The phantoms were scanned on a 64-section CT machine (SOMATOM Definition AS 64; Siemens AG, Healthcare Sector, Forchheim, Germany) with a single-source scan protocol (software version VA44). The ratio between the quality reference milliampere second at low and high kilovolt (peak) is fixed at 4.25, which results in similar image noise for both voltage levels. The 2 phantoms were scanned once with each inlay with the following scan parameters: tube voltage pair, 80/140 kV(p); tube current-time product, 133/32 effective mAs (30 cm) and 461/85 effective mAs (40 cm) with attenuation-based tube current modulation (CAREDose4D; Siemens); pitch, 0.6; gantry rotation time, 0.5 seconds; slice collimation, 64 × 0.6 mm. These protocol parameters were associated with volume CT dose index values of 6.6 mGy for the 30-cm phantom and 19.7 mGy for the 40-cm phantom. One additional scan was performed in the 30-cm phantom with movement (along the *z* axis) of the renal phantom between the 80- and the 140-kV(p) acquisition for simulating patient movement with the same scan parameters mentioned previously. The movement was performed with a maximum amplitude of 2 cm in each direction.

Data were reconstructed with the default reconstruction algorithm (FBP) using a medium soft-tissue convolution kernel for dual-energy (D30f) and with sinogram-affirmed IR (SAFIRE; Siemens Healthcare, Forchheim, Germany) with a dual-energy IR kernel (Q30f) using a strength level of 3 (as recommended by the manufacturer). Images were reconstructed with a section thickness of 1.5 mm and 1.0-mm increment. Mixed images (weighting factor, 0.3) from the 80- and 140-kV(p) acquisition and further results were calculated after applying the motion correction algorithm for coregistration. This algorithm handles object deformation between both image sets and different absolute CT values as encountered in dual-energy CT.[20]

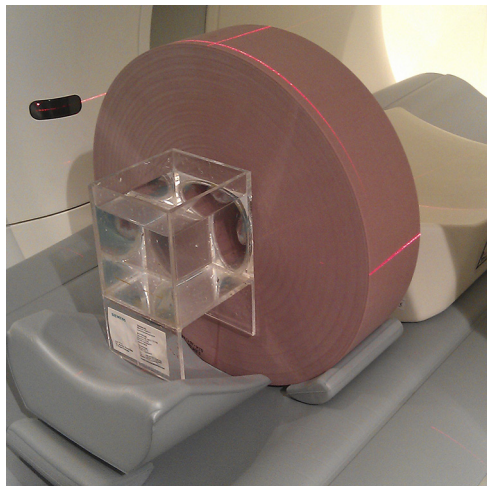

FIGURE 1. Photograph of the water-equivalent cylindrical phantom (diameter, 40 cm) with the aperture for changing the kidney phantoms.

X-ray Diffraction

X-ray diffraction was used to determine the chemical composition of the stones before CT scanning was performed. A sample of each urinary stone was crushed and analyzed by x-ray diffraction using a diffractometer (CubixPro; PANalytical, Almelo, the Netherlands) with Ni-filtered CuK radiation. The identification of the crystalline components was performed using the international center for diffraction data database and the semiquantitative composition determined using the relative intensity of the different bands.

Qualitative Image Evaluation

Qualitative image evaluation was performed on a high-definition liquid crystal display monitor (BARCO-Medical Imaging Systems, Kortrijk, Belgium) using the picture archiving and communication system (IMPAX, version 6.4.0.4551; Agfa-Gevaert, Mortsel, Belgium) of our hospital. Two readers (R1 and R2, both with 3 years of experience in abdominal imaging), blinded to the stone number, location, and composition, scrolled through the mixed images of the FBP and IR data sets with the 30- and 40-cm phantoms. Window settings were fixed (center, 300; width 40). When a stone was detected, the slice number was noted to allow the readers for correctly identifying stones on other data sets.

The readers graded the overall image quality of the entire data set on a 4-point Likert scale[21]: score 4, very acceptable; score 3, acceptable; score 2, marginally to fairly acceptable; and score 1, not acceptable. In addition, the visibility of each stone was rated as follows[21]: score 4, clearly delineated; score 3, moderately visualized; score 2, marginally to fairly delineated; and score 1, not able to be depicted acceptably.

Quantitative Image Evaluation

Image noise was measured as the standard deviation of a 5-cm^2–sized circular region of interest placed in the water part of the phantom body by R1.

In addition, R1 manually drew a freehand region of interest in the stones encompassing at least 80% of the stone using the 80- and 140-kV(p) data sets. Stone composition was also determined on the color-coded images on a workstation (MultiModality Workplace, version VE52A; Siemens AG, Healthcare Sector) equipped with a commercially available postprocessing software (syngo Dual Energy; Siemens AG, Healthcare Sector). This software includes a motion correction algorithm[20] and an algorithm that calculates the characteristic ratio (ratio = [CT value_voxel,low − CT value_kidney,low]/[CT value_voxel,high − CT value_kidney,high]) and color-codes the stones. The stones were classified as UA-containing stones when the ratio was lower than 1.15 and the stones were colored red. The stones were classified as non–UA-containing when the ratio was higher than 1.15 and the stones were colored blue.

Statistical Analysis

Data analysis was performed using a commercially available software (Statistical Package for the Social Sciences Statistics version 20, release 20.0.0; IBM, Chicago, IL). Variables are expressed as mean (SD).

The interreader agreement regarding the qualitative evaluation was analyzed by using the Cohen κ. According to Landis and Koch,[22] κ values of 0.61 to 0.80 were interpreted as substantial agreement; 0.81 to 1.00, as high agreement.

The Wilcoxon signed rank test was used to compare the data sets reconstructed with FBP and IR.

The Student *t* test for paired samples was used to compare noise between the data sets reconstructed with FBP and IR.

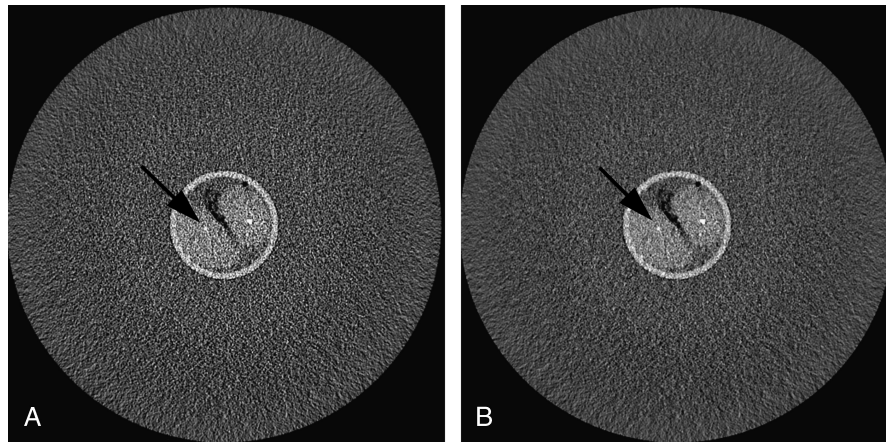

FIGURE 2. Transverse images of the 40-cm abdominal phantom depicting 2 UA-containing stones (at a window of 300 [width] and 40 [level]). The smaller UA-containing stone (black arrow) was rated as having a higher visibility on the IR (B) as compared with the FBP reconstructed images (A).

The dual-energy index (DEI) was calculated for each stone with the previously described formula: $DEI = (HU_{80kV(p)} - HU_{140kV(p)})/(HU_{80kV(p)} + HU_{140kV(p)} + 2000\ HU)$.[8]

The Hounsfield unit (HU) ratio was calculated for each stone using the formula given previously. The advantage of this formula is that partial volume effects are suppressed by assuming only 1 other material in the neighborhood of the stone.

The analysis of variance was used to compare the DEI between UA stones, cystine, and struvite stones as well as stones containing calcium (eg, whewellite).

The Friedman test was used to test for differences in stone size measurements between the data sets and the criterion standard method.

A P value less than 0.05 was considered statistically significant.

RESULTS

Stone Characterization

On the basis of the results from x-ray diffraction, the stones types were as follows: 29 pure composition stones (10 UA stones, 8 cystine stones, 4 apatite stones, 3 whewellite stones, 2 struvite stones, 2 brushite stones) and 6 stones with mixed composition (4 containing >70% UA stones; 2 non-UA stones).

The long-axis diameter measured with the precision caliper ranged between 2.9 and 13.8 mm with a mean value of 6.4 mm.

Qualitative Evaluation

Both readers detected all stones on all data sets, resulting in 140 observations per reader. Interreader agreement was high concerning the overall image quality ($\kappa = 0.875$, $P < 0.001$) and visibility of the stones ($\kappa = 0.810$, $P < 0.001$).

The readers found a similar overall image quality for the 30-cm phantom when comparing FBP with the IR data sets (R1: 3.8 vs 4, $P = 0.317$; R2: 4 vs 4, $P = 1$). In the 40-cm phantom, the overall image quality was rated higher by both readers in the IR data sets (R1: 3.0 vs 4.0, $P = 0.025$; R2: 3.2 vs 4.0, $P = 0.046$).

The visibility of stones was rated significantly higher for both the 30-cm phantom (FBP vs IR; R1: 3.7 vs 3.9, $P = 0.005$; R2: 3.7 vs 3.9, $P = 0.008$) and the 40-cm phantom (FBP vs IR; R1: 3.5 vs 3.9, $P < 0.001$; R2: 3.5 vs 3.8, $P = 0.002$) with IR as compared with FBP. This improvement was further pronounced when analyzing only the visibility of UA-containing stones (30-cm phantom: FBP vs IR; R1: 3.4 vs 3.9, $P = 0.008$; R2: 3.4 vs 3.8, $P = 0.014$; 40-cm phantom: FBP vs IR; R1: 3.2 vs 3.9, $P = 0.003$; R2: 3.2 vs 3.7, $P = 0.008$) (Fig. 2).

Quantitative Evaluation

Noise was significantly reduced by 28% in the 30-cm phantom (28.1 HU vs 20.4 HU, $P = 0.003$) and by 31% in the 40-cm phantom (46.1 HU vs 31.6 HU, $P < 0.001$) in the IR as compared with the FBP data sets. There were no significant differences ($P > 0.05$) in stone sizes between the various data sets and the criterion standard measurements (Table 1).

There were no significant differences between DEI in the FBP and IR data sets for the 30-cm phantom (0.052 vs 0.055, $P = 0.116$) and for the 40-cm phantom (0.048 vs 0.047, $P = 0.544$). Dual-energy index was significantly ($P < 0.001$) different between UA-containing stones, cystine and struvite stones, as well as stones of other compositions (Table 2; Fig. 3). This was true for all data sets.

An HU ratio of 1.15 for the 80- and 140-kV(p) scans could discriminate accurately between UA- and non-UA–containing stones (Fig. 4).

Software-Based Stone Discrimination

All stones on all data sets, including the scans with motion in between scans, were classified correctly as UA- or non–UA-containing urinary stones. In the 40-cm phantom, falsely colored voxels appeared in the FBP data sets where no stones were placed in the renal phantom. The reason is that image noise randomly exceeds

TABLE 1. Urinary Stone Sizes Measured With a Precision Caliper and on the Various Data Sets

	UA Stones	Cystine/Struvite Stones	Calcified Stones
True stone size, mm	5.1 (1.6)	6.5 (2.4)	8.0 (2.8)
30-cm phantom - FBP, mm	5.0 (1.4)	6.7 (2.7)	7.8 (3.0)
30-cm phantom - IR, mm	5.0 (1.4)	6.7 (2.8)	7.8 (3.1)
40-cm phantom - FBP, mm	4.9 (1.3)	6.7 (2.8)	7.8 (3.2)
40-cm phantom - IR, mm	4.8 (1.4)	6.4 (2.7)	7.7 (3.3)

All values are expressed as mean (SD).

FBP indicates filtered back projection; IR, iterative reconstruction.

TABLE 2. Dual-Energy Indices Between the Various Stone Types and Phantoms

	DEI UA Stones	DEI Cystine/Struvite Stones	DEI Calcified Stones	*P*
30-cm phantom - FBP	0.005 (0.012)	0.061 (0.012)	0.105 (0.017)	<0.001
30-cm phantom - IR	0.005 (0.011)	0.063 (0.013)	0.111 (0.022)	<0.001
40-cm phantom - FBP	0.002 (0.015)	0.059 (0.017)	0.095 (0.023)	<0.001
40-cm phantom - IR	0 (0.014)	0.060 (0.019)	0.097 (0.019)	<0.001

All values are expressed as mean (SD).

DEI indicates dual-energy index; FBP, filtered back projection; IR, iterative reconstruction; UA, uric acid.

the color-coding threshold of 200 HU for such a large object. These falsely colored voxels disappeared when using IR as the reconstruction technique (Fig. 5).

DISCUSSION

This ex vivo study is the first, to the best of our knowledge, to test a single-source dual-energy protocol that applies sequential data acquisition of the 2 energy levels and a coregistration motion correction algorithm for urinary stone characterization. Our results indicate that such a single-source dual-energy CT protocol is feasible and allows for an accurate characterization and differentiation of different urinary stone types using a conventional single-source CT scanner. In addition, we introduced IR for dual-energy CT imaging, demonstrating its value in improving image quality, visualization, and classification of urinary stones, an effect that was found primarily in the phantom simulating patients with obesity.

Attempts for differentiating urinary stone types with dual-energy imaging using 2 consecutive scans at 2 different energy levels with single-source CT have been undertaken more than a decade ago.[23,24] For example, Boulay et al[25] and Mostafavi et al[26] showed promising initial results in their in vitro studies using phantoms with urinary stones. However, an in vivo study by Grosjean et al[27] showed that when slight motion was applied to renal stones during image acquisition, the HU values become significantly different from those obtained without motion, rendering an accurate differentiation of urinary stones impossible. This problem of misregistration was overcome in 2006 by the introduction of dual-source CT enabling simultaneous acquisition of images at 2 x-ray spectra.[28] In the meantime, several ex vivo and in vivo studies demonstrated good performance characteristics of the dual-source dual-energy CT approach for differentiating various stone types.[6–10]

More recently, the rapid kilovolt (peak)–switching approach has become feasible for dual-energy CT, in which the generator switches between 80- and 140-kV(p) energy levels in less than 0.5 milliseconds. Using this approach, Kulkarni et al[11] showed that rapid kilovolt (peak) switching can help in the differentiation between different stone types both in vitro and in vivo.

Importantly, both of these approaches require a dedicated scanner hardware specifically designed for dual-energy CT data acquisition. Our results add to the current dual-energy CT literature by introducing a scan protocol on a conventional single-source CT machine with consecutive, sequential CT data acquisition at the 2 energy

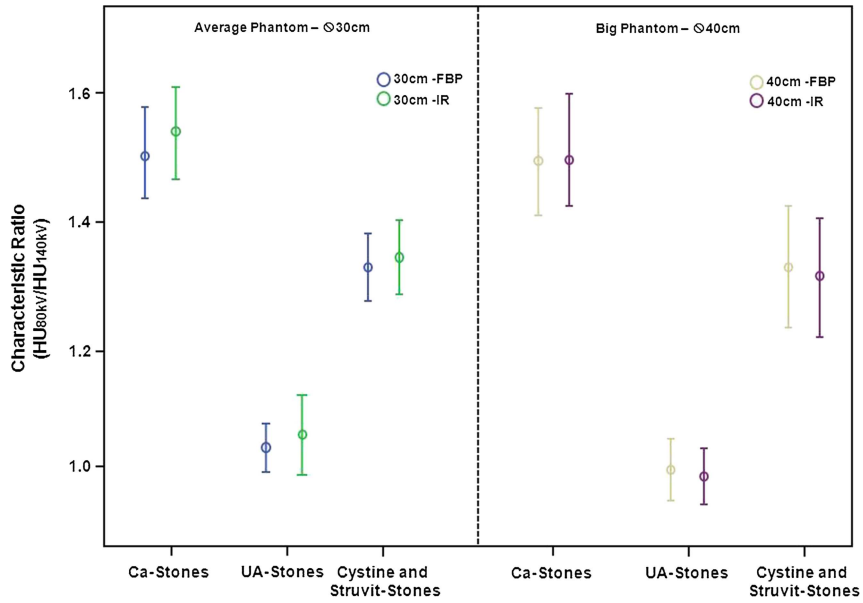

FIGURE 3. Bar graphs demonstrating the dual-energy ratios (whiskers representing 95% confidence intervals of calcified stones [Ca] and UA-containing stones, as well as those of cystine and struvite stones). Note the similar discriminative capability of the images reconstructed with FBP and with IR for the various stone types.

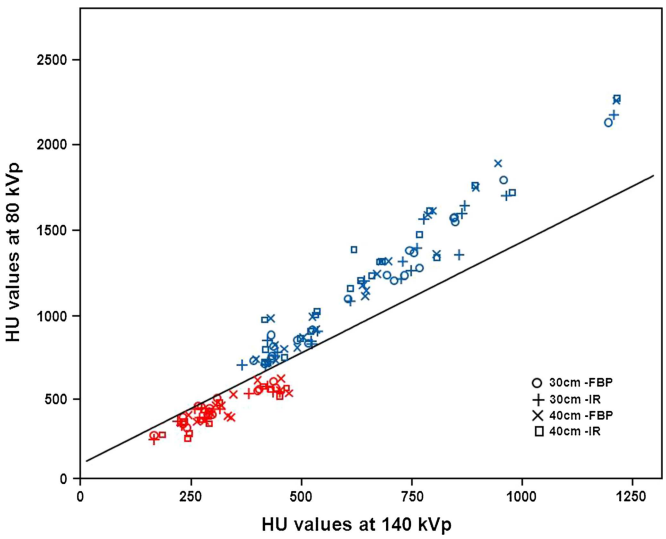

FIGURE 4. Scatterplot depicting attenuation values (in Hounsfield units) of individual stones measured on the 80- and 140-kV(p) data sets for both phantom sizes. Diagonal line differentiates between UA- (red) and non–UA-containing (blue) stones.

levels, along with the coregistration for correcting potential motion artifacts between scans. Using this approach, we were able to differentiate urinary stones with similar accuracy as compared with that of previously published studies,[6–11] despite movement of the phantom to mimic patient motion between scans.

Iterative reconstruction algorithms have been proven useful in clinical routine because they increase image quality and have the potential for dose reduction.[13–16] In line with the literature, we found that IR results in improved image quality particularly in our phantom simulating patients with obesity (with 40-cm diameter). In addition, the overall stone visualization was improved with IR, especially for UA-containing stones in the large phantom. Image noise was reduced by up to 31% as compared with FBP reconstruction images, which is in concordance with previously published noise reduction levels achieved with IR.[13–16]

Some of the previous dual-energy CT studies revealed shortcomings regarding image quality and accuracy in patients with abdominal obesity.[17–19] The explanation of this is thought to be the higher level of image noise particularly at the low tube voltage level. Our study indicates that the use of IR can improve the image quality by reducing noise, a beneficial effect that we observed particularly in the large phantom. Moreover, the use of IR did not affect the accuracy of HU value measurements and, hence, that of stone characterization. Constancy of attenuation values when using IR has been previously described also by Kalra et al,[29] who showed similar HU values compared with FBP reconstruction data sets. In our study, IR also helped to avoid erroneous classification of image mottle as small urinary stones (Fig. 5).

It is important to note that the sequential acquisition used herein did not result in a doubling of radiation dose as compared with a single data acquisition. Our volume CT dose index values were in the range of 6.6 to 19.7 mGy, which are similar to those previously reported using the dual-source (11.9–22.6 mGy[6,8,17]) and the rapid kilovolt (peak)–switching approach (19.11–29.2 mGy[11,12]). Thus, dual-energy CT appears feasible with sequential data acquisition using a single-source CT scanner without a dose penalty as compared with previous techniques.

Some study limitations need to be addressed. First, the inherent shortcomings of an ex vivo study must be acknowledged and validation of our results in a prospective patient series is needed. Second, we used a limited number of mixed stones consisting of stones with a predominant stone composition. Third, the distribution of stones in our ex vivo experiments might not represent the normal prevalence of urinary stones in patients.[30] Fourth, we did not move our phantom continuously, which might have resulted in an overestimation of the quality of the coregistration algorithm used. Fourth, we did not test the maximum amplitude of movement, which would allow a flawless stone characterization. Fifth, we analyzed movement only in the normal-weight phantom. Finally, we did not investigate the potential of IR for dose reduction but only showed that the technique can be used for improving image quality of dual-energy data at the same radiation dose level.

In conclusion, DECT is feasible also with a conventional single-source CT machine when equipped with software allowing for sequential data acquisition at the 2 energy levels and a coregistration motion correction algorithm. It then allows for an accurate differentiation of urinary stones of various compositions. Iterative reconstruction can be used in DECT without a loss in image

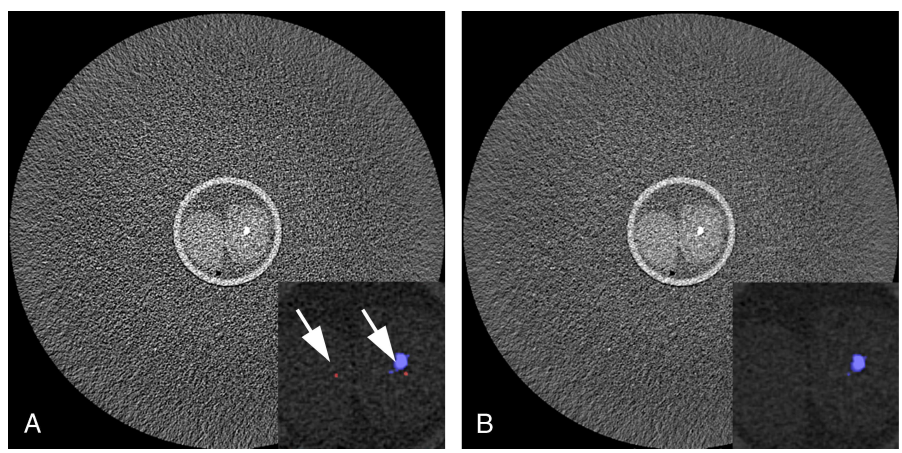

FIGURE 5. Transverse images of the 40-cm abdominal phantom depicting a struvite stone. A, Note 2 falsely colored voxels on the FBP images (weighted image, large; arrows on the color-coded image, insert), which were no longer present when using IRs (B).

information, resulting in a further improvement in image quality and visibility of urinary stones, particularly in large body diameters.

REFERENCES

1. Smith RC, Levine J, Dalrymple NC, et al. Acute flank pain: a modern approach to diagnosis and management. *Semin Ultrasound CT MR*. 1999;20:108–135.
2. Smith RC, Rosenfield AT, Choe KA, et al. Acute flank pain: comparison of non-contrast-enhanced CT and intravenous urography. *Radiology.* 1995; 194:789–794.
3. Kambadakone AR, Eisner BH, Catalano OA, et al. New and evolving concepts in the imaging and management of urolithiasis: urologists' perspective. *Radiographics*. 2010;30:603–623.
4. Motley G, Dalrymple N, Keesling C, et al. Hounsfield unit density in the determination of urinary stone composition. *Urology.* 2001;58:170–173.
5. Nakada SY, Hoff DG, Attai S, et al. Determination of stone composition by noncontrast spiral computed tomography in the clinical setting. *Urology.* 2000;55:816–819.
6. Stolzmann P, Leschka S, Scheffel H, et al. Characterization of urinary stones with dual-energy CT: improved differentiation using a tin filter. *Invest Radiol*. 2010;45:1–6.
7. Boll DT, Patil NA, Paulson EK, et al. Renal stone assessment with dual-energy multidetector CT and advanced postprocessing techniques: improved characterization of renal stone composition—pilot study. *Radiology.* 2009;250: 813–820.
8. Graser A, Johnson TR, Bader M, et al. Dual energy CT characterization of urinary calculi: initial in vitro and clinical experience. *Invest Radiol*. 2008;43: 112–119.
9. Matlaga BR, Kawamoto S, Fishman E. Dual source computed tomography: a novel technique to determine stone composition. *Urology.* 2008;72: 1164–1168.
10. Stolzmann P, Kozomara M, Chuck N, et al. In vivo identification of uric acid stones with dual-energy CT: diagnostic performance evaluation in patients. *Abdom Imaging*. 2010;35:629–635.
11. Kulkarni NM, Eisner BH, Pinho DF, et al. Determination of renal stone composition in phantom and patients using single-source dual-energy computed tomography. *J Comput Assist Tomogr*. 2013;37:37–45.
12. Li B, Yadava G, Hsieh J. Quantification of head and body CTDI(VOL) of dual-energy x-ray CT with fast-kVp switching. *Med Phys*. 2011;38:2595–2601.
13. Desai GS, Uppot RN, Yu EW, et al. Impact of iterative reconstruction on image quality and radiation dose in multidetector CT of large body size adults. *Eur Radiol*. 2012;22:1631–1640.
14. Prakash P, Kalra MK, Kambadakone AK, et al. Reducing abdominal CT radiation dose with adaptive statistical iterative reconstruction technique. *Invest Radiol*. 2010;45:202–210.
15. May MS, Wust W, Brand M, et al. Dose reduction in abdominal computed tomography: intraindividual comparison of image quality of full-dose standard and half-dose iterative reconstructions with dual-source computed tomography. *Invest Radiol*. 2011;46:465–470.
16. Baumueller S, Winklehner A, Karlo C, et al. Low-dose CT of the lung: potential value of iterative reconstructions. *Eur Radiol*. 2012;22:2597–2606.
17. Scheffel H, Stolzmann P, Frauenfelder T, et al. Dual-energy contrast-enhanced computed tomography for the detection of urinary stone disease. *Invest Radiol*. 2007;42:823–829.
18. Qu M, Jaramillo-Alvarez G, Ramirez-Giraldo JC, et al. Urinary stone differentiation in patients with large body size using dual-energy dual-source computed tomography. *Eur Radiol*. 2013;23:1408–1414. doi: 10.1007/s00330-012-2727-4.
19. Thomas C, Heuschmid M, Schilling D, et al. Urinary calculi composed of uric acid, cystine, and mineral salts: differentiation with dual-energy CT at a radiation dose comparable to that of intravenous pyelography. *Radiology.* 2010;257:402–409.
20. G Hermosillo CC, Herrmann K-H, Bousquet G, et al. Image registration in medical imaging: applications, methods, and clinical evaluation. In: El-Baz AS, Acharya UR, Laine AF, et al, eds. *Multi Modality State-of-the-Art Medical Image Segmentation and Registration Methodologies.* Vol 2. Springer; 2011:263–313.
21. Paulson EK, Weaver C, Ho LM, et al. Conventional and reduced radiation dose of 16-MDCT for detection of nephrolithiasis and ureterolithiasis. *AJR Am J Roentgenol*. 2008;190:151–157.
22. Landis JR, Koch GG. The measurement of observer agreement for categorical data. *Biometrics*. 1977;33:159–174.
23. Hawkes DJ, Jackson DF, Parker RP. Tissue analysis by dual-energy computed tomography. *Br J Radiol*. 1986;59:537–542.
24. Marshall WH Jr, Alvarez RE, Macovski A. Initial results with prereconstruction dual-energy computed tomography (PREDECT). *Radiology.* 1981;140: 421–430.
25. Boulay I, Holtz P, Foley WD, et al. Ureteral calculi: diagnostic efficacy of helical CT and implications for treatment of patients. *AJR Am J Roentgenol*. 1999;172:1485–1490.
26. Mostafavi MR, Ernst RD, Saltzman B. Accurate determination of chemical composition of urinary calculi by spiral computerized tomography. *J Urol*. 1998;159:673–675.
27. Grosjean R, Sauer B, Guerra RM, et al. Characterization of human renal stones with MDCT: advantage of dual energy and limitations due to respiratory motion. *AJR Am J Roentgenol*. 2008;190:720–728.
28. Flohr TG, McCollough CH, Bruder H, et al. First performance evaluation of a dual-source CT (DSCT) system. *Eur Radiol*. 2006;16:256–268.
29. Kalra MK, Woisetschlager M, Dahlstrom N, et al. Radiation dose reduction with sinogram affirmed iterative reconstruction technique for abdominal computed tomography. *J Comput Assist Tomogr*. 2012;36:339–346.
30. Coe FL, Evan A, Worcester E. Kidney stone disease. *J Clin Invest*. 2005;115: 2598–2608.